

Investigation of the Impact of Random Dopant Fluctuation on Static Noise Margin of 22nm SRAM

Sarah Q. Xu

*School of Electrical and Computer Engineering
Cornell University
Ithaca, NY, USA
qx33@cornell.edu*

Kai Xiu and Phil Oldiges

*Semiconductor Research and Development Center,
Systems and Technology Group
IBM Corporation
Hopewell Junction, NY, USA*

Abstract— In this paper, the impact of RDF on the static noise margin (SNM) and read current margin (SINM) of a prototype 22nm 6T SRAM was investigated using TCAD modeling. Individual device statistics of threshold voltages (V_t) and transport related parameters were first extracted for NFETs and PFETs. SNM and SINM characteristics of the corresponding SRAM cells were then analyzed. Two methods to emulate the impact of RDF were simulated — modulating gate work function, and uniform scaling of the continuum dopant distribution. Compared to RDF devices, both methods underestimated V_t and SNM variations.

Keywords—Random dopant fluctuation (RDF), SRAM, static noise margin (SNM), read current noise margin (SINM), threshold voltage variation.

I. INTRODUCTION

Driven by the improvements on performance and cost of today's integrated circuits, new generations of SRAM cells are being aggressively scaled down to 22nm technology node and beyond [1]. Continued advancement of the complementary metal oxide semiconductor (CMOS) technologies reduce the feature sizes closer to atomic dimensions, lowering supply voltage and power consumption. Cells and systems based on such devices are becoming more susceptible to variations and mismatches, causing various scaling challenges [2]. One of the most pronounced scaling effect is the threshold voltage (V_t) variations caused by random dopant fluctuation (RDF) in the channel region [3, 4].

RDF effect refers to the microscopic variations in the discrete number and arrangement of the channel dopant as device feature shrinks down dramatically [5, 6]. The effect was first explored in the seventies [4], and later recognized to be the major contributor to device variations at sub-100nm dimensions [7, 8]. Since RDF is entirely intrinsic and cannot be eliminated through careful control of the fabrication process, it has become the functionality bottleneck for minimum-feature device, such as area-constrained SRAM cells [9].

In this study, dopant fluctuations were introduced into a prototype 22nm 6T SRAM cell using Monte Carlo techniques. The statistics of threshold voltages and transport related

parameters of individual devices were first extracted and presented in section II. SNM and SINM characteristics of the corresponding SRAM cells were then analyzed using mixed mode simulation and summarized in section III. Two alternative approaches—gate work function modulation, and uniform scaling of the continuum dopant distribution—were also studied to assess how well they can emulate the impact of RDF.

II. INDIVIDUAL DEVICE SIMULATION

Figure 1 illustrates the cross section of a prototype 22nm planar device employed in this study, with an instance of RDF doping profile. Statistical characteristics were analyzed individually for Pull-down (PD) NFET, Pull-up (PU) PFET, and Pass-gate (PG) NFET. Process simulations were performed in TSUPREM-4 [10] using a prototype process flow to generate the nominal device structures. RDF was then introduced into the nominal structure with Monte Carlo simulated doping profiles assuming Poisson distributions for the dopants. The resulting linear and saturation threshold voltage distributions of PD NFET are shown in Figure 2 as an example. The structure parameters and the corresponding statistical V_t results of all three types of devices are summarized in Table 1. As device width shrinks down, the amount of channel dopant drops, making the device-to-device fluctuations in discrete doping profile more prominent. Therefore, PU PFET, with the smallest geometries and dopant number, shows the largest threshold voltage variation (σV_t) among the three.

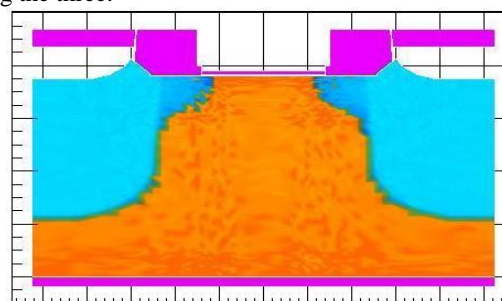


Figure 1 Cross section of the prototype 22nm NFET device with an instance of random dopant fluctuation in the channel

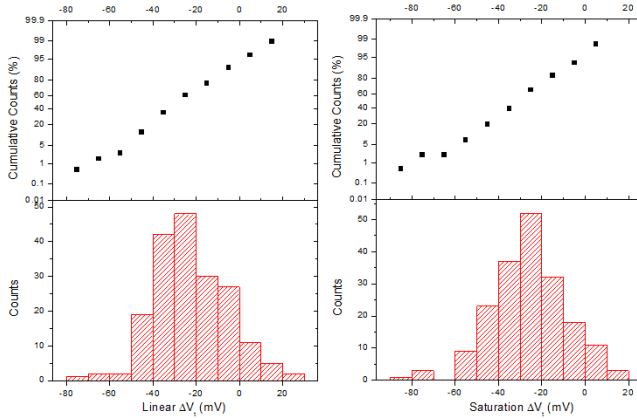


Figure 2 a) linear threshold voltage distribution b) saturation threshold voltage distribution of RDF Pull-down NFETs referenced to nominal device results

TABLE 1

Standard deviations of threshold voltages for RDF devices at both linear ($\sigma_{V_{tlin}}$) and saturation ($\sigma_{V_{tsat}}$) regions using a sample size of 200.

Device	Width	$\sigma_{V_{tlin}}$ (mV)	$\sigma_{V_{tsat}}$ (mV)
Pull Down NFET	8L	16.6	17.6
Pass Gate NFET	5L	17.5	17.6
Pull Up PFET	3L	28.4	36.7

Two alternative approaches were investigated to understand how well the effect of RDF could be emulated without using discrete doping profiles. Gate work function modulation (WF) and continuum channel dopant scaling (Continuum) were performed. Threshold voltage variations were extracted for all three devices using both methods.

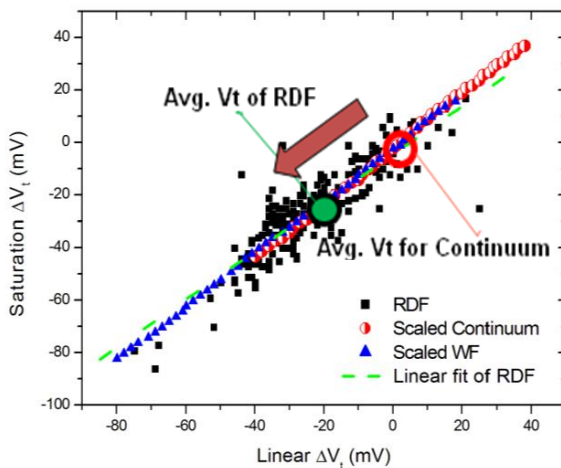


Figure 4 Saturation ΔV_t vs linear ΔV_t referenced to the nominal device values for all three devices: RDF, Continuum and WF. An average V_t shift was observed between RDF devices and Continuum devices.

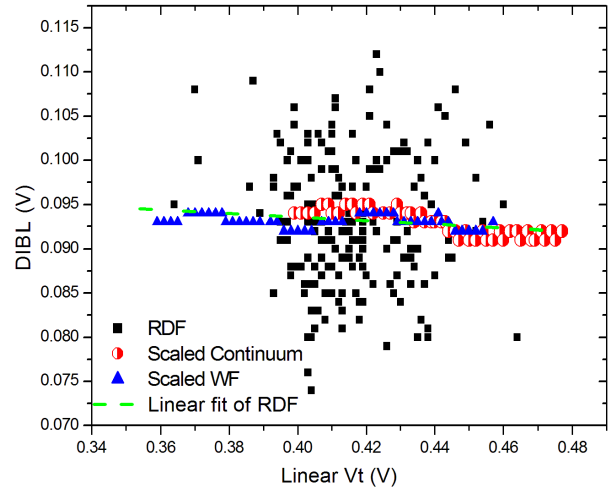


Figure 5 DIBL vs linear ΔV_t for all three cases. DIBL of WF devices only showed 1mV fluctuations which was caused by the granularity of data extraction.

Gate work function scaling captures σV_t of RDF effect by varying the gate work function of the nominal device, so that the resulting threshold voltage range is the same as that of the simulated RDF devices. This is the most intuitive way to imitate the threshold voltage variations in RDF without considering the doping number or location in the channel. Scaling the channel dopant (Continuum), on the other hand, accounts for the differences in the number of channel dopants; however, it does not consider the discreteness of the dopant or the random dopant arrangement in space.

The linear/saturation V_t and carrier transport related properties such as drain-induced barrier lowering (DIBL) and overdrive current (I_{odlin}) were summarized in Figure 4, 5 and 6 respectively. Since DIBL and R_{on} are affected by doping variations, Continuum devices captured DIBL/ R_{on} better than WF devices.

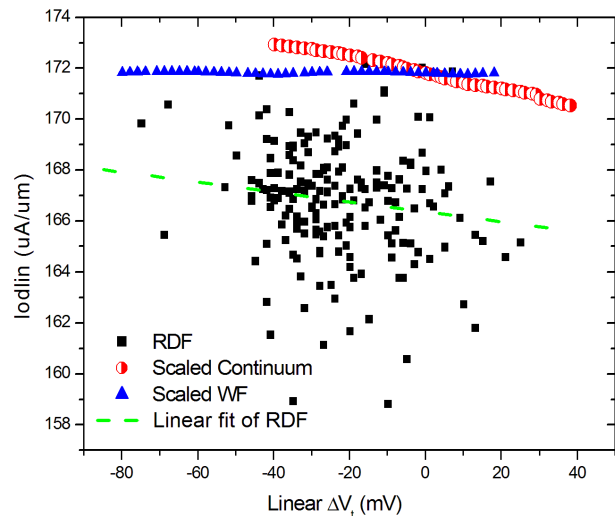


Figure 6 Linear overdrive current vs linear ΔV_t . WF devices showed no V_t dependency due to unvaried channel doping profile.

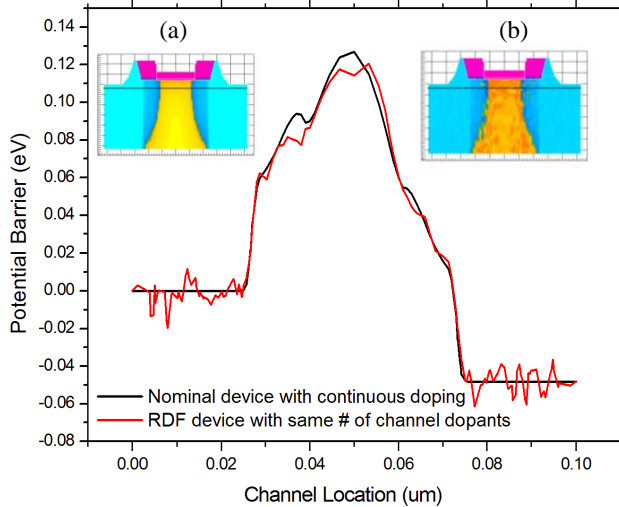


Figure 7 Potential barrier at threshold voltage bias for nominal and RDF devices having the same number of channel dopant. Inserts: example of a) nominal and b) RDF device doping profile.

In addition, a shift in V_t exists between the Continuum and RDF devices, which is evident in Figure 4. This phenomenon was first observed in [7], where the average shift of the threshold voltage was attributed to the inhomogeneity of channel potential due to the randomness and discreteness of the channel dopants. In Figure 7, an instance of potential barrier vs channel location was graphed out for the nominal and RDF devices having the same number of channel dopants at threshold voltage bias. It is clear to see that due to the random dopant distribution, the potential barrier profile of the RDF device fluctuates along the channel region, causing the maximum barrier height to be lower than that of the Continuum device, in spite of the fact that they have the same number of channel dopants.

III. MIXED MODE SIMULATION

The stability and reliability of SRAM cells during read and write operations are often characterized by the noise margins that need to be maintained [9, 11]. The benchmarks for accessing the SRAM cell stability are usually the static noise margin (SNM) and current noise margin (SINM) during read operation [4, 5, 6], during which the cell states are most vulnerable to external signal perturbations. SNM is the maximum tolerable DC noise voltage at a storage node without causing a read disturbance, while SINM is determined from an N-curve measurement [12].

In the mixed mode simulation, RDF, WF and Continuum devices are used individually to create their corresponding SRAM groups. For RDF SRAMs, each of PD, PG and PU contributes 200 devices into the device selection pool with a naturally Gaussian distribution in V_t due to the Monte Carlo generated doping profiles, and the devices are then randomly selected to form the desired SRAM cells. The WF device pool was created by using the nominal device threshold voltage as

the average V_t , and the RDF σV_t was used to calculate the range of work function required. The WF SRAM cells were then randomly selected from the device pool with the same Gaussian probability seen in the RDF devices. Instead of matching the σV_t , the Continuum devices used the nominal device doping profile as the average device doping profile, and the RDF dopant distribution to obtain the range of amount of channel dopant required. Again, the dopant numbers follow the same distribution as the RDF case.

22nm 6T SRAMs were then set up using RDF, Continuum, or WF devices. The SNM and SINM were simulated using sample size of 1000; statistic results are illustrated in Figure 8. It is interesting to see that, in spite of the fact that only Continuum devices were able to capture DIBL and R_{on} variations, SRAMs built using Continuum and WF devices showed similar distribution in SNM and SINM; however, neither of the simpler methods predicted the same results as that of the RDF cells.

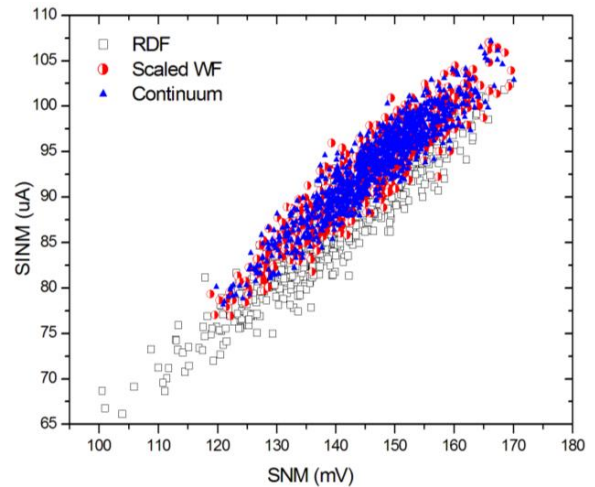


Figure 8 SRAMs composed of WF and Continuum devices show similar SNM and SINM, and both are larger than RDF cells.

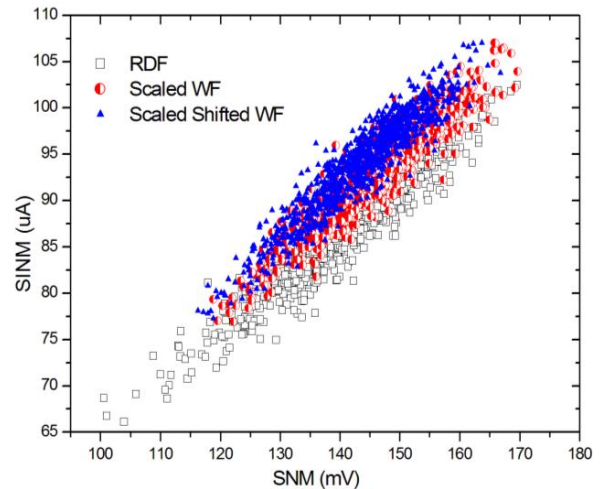


Figure 9 SNM and SINM for SRAMs composed of RDF, WF and Shifted WF devices. Shifted WF cannot emulate the RDF behavior.

TABLE 2

a) SNM and b) SINM variations for SRAMs composed of RDF, Continuum, WF and shifted WF devices.

(a)		
SRAM device	σ_{SNM} (mV)	SoS of SNM (mV)
RDF	10	Approximately 0.20
Continuum	8.6	
WF	8.7	
Shifted WF	8.5	

(b)		
SRAM device	σ_{SINM} (μA)	SoS of SINM (μA)
RDF	5.6	Approximately 0.10
Continuum	5	
WF	5.1	
Shifted WF	5.22	

In addition, since there is an average threshold voltage shift between the mean RDF and the nominal device, the comparison between RDF and the other two cases may be distorted. In order to eliminate the contribution from this average V_t shift and focus only on the RDF effect, a new group of SRAM cells having the same average V_t as RDF was simulated. Since previously WF and Continuum sets are seen to show similar results in SNM and SINM variations, shifted WF devices were chosen over shifted channel doping devices to investigate this effect for a simpler simulation scheme. The results are shown in Figure 9. With lower V_t , shifted WF devices showed a slightly smaller SNM and larger SINM; however, σ_{SNM} and σ_{SINM} remained the same as the original WF SRAMs. The results indicate that shifting the average threshold voltage without considering the dopant distribution cannot recreate the RDF results. Standard deviation of the standard deviation (SoS) is used to evaluate the difference in variations among the four cases to assess if they are significant enough to be seen as statistically different. Shifted WF SRAMs, despite having the same average V_t and σV_t as the RDF devices, still have a smaller standard deviation. The SoS confirms that the differences among of the four SRAM sets are significant (over 3σ), as seen in Table 2.

IV. CONCLUSION

TCAD modeling of RDF impact on a prototype 22nm 6T SRAM is presented in this paper. Statistics of V_t variations and transport related parameters were obtained for individual types of devices. Two methods to emulate the RDF effect were investigated—scaling of the continuum dopant distribution, and gate work function modulation. Since the Continuum devices contained some channel doping

information, they were able to capture DIBL and R_{on} better than WF devices, however, neither could reproduce the RDF effect adequately. Mixed mode simulations were then employed to simulated 6T SRAM cells composed of three different types of devices, and the corresponding SNM and SINM characteristics were extracted. Continuum and WF devices showed similar SNM/ σ_{SNM} and SINM/ σ_{SINM} , in spite of the fact that Continuum devices were able to deliver DIBL & R_{on} variations. From a statistical point of view, in order to accurately examine the effect of random dopant fluctuations within the 22nm SRAM cell, full scale Monte Carlo simulated doping profile is necessary. WF and Continuum devices are only capable of showing the general trend, but neither method was seen to emulate the RDF effect satisfactorily.

ACKNOWLEDGMENT

The authors would like to thank Xin Wang from IBM and Edwin C. Kan from Cornell University for fruitful discussions and useful feedback.

REFERENCES

- [1] International Technology Roadmap for Semiconductors (ITRS), 2011
- [2] K.J.Kuhn, "Reducing variation in advanced logic technologies: Approaches to process and design for manufacturability of nanoscale CMOS," *IEDM Tech. Dig.*, pp. 471–474, Dec. 2007
- [3] R. W. Keyes, "The effect of randomness in the distribution of impurity atoms on FET thresholds," *Appl. Phys.*, vol. 8, pp. 251–259, 1975
- [4] D. J. Frank, Y. Taur, M. Jeong, and H.-S. P. Wong, "Monte Carlo modeling of threshold variation due to dopant fluctuations", *Symp. VLSI Technol. Dig.*, pp.169 -170 1999
- [5] X. Tang, V. De and J. Meindl "Intrinsic MOSFET parameter fluctuations due to random dopant placement", *IEEE Trans. VLSI Syst.*, vol. 5, pp.369 1997
- [6] B. Cheng , S. Roy and A. Asenov "The impact of random doping effects on CMOS SRAM cell", *Proc. Eur. Solid-State Circuits Conf.*, pp.219 2004
- [7] H. S. Wong and Y. Taur, "Three-dimensional atomistic simulation of discrete random dopant distribution effects in sub-0.1 μm MOSFET's", *IEDM Tech. Dig.*, pp. 705, 1993
- [8] A. Asenov "Random dopant induced threshold voltage lowering and fluctuations in sub", *IEEE Trans. Electron Devices*, vol. 45, pp.2505 1998
- [9] A. Bhavnagarwala , X. Tang and J. Meindl "The impact of intrinsic device fluctuations on CMOS SRAM cell stability", *IEEE J. Solid-State Circuits*, vol. 36, pp.658 2001
- [10] Synopsys, Inc., TSUPREM-4, Two-Dimensional Device Simulation Program Version Version D-2-1-.03 User's Manual
- [11] D. Burnett, K. Erington, C. Subramanian, and K. Baker, "Implications of fundamental threshold voltage variations for high-density SRAM and logic circuits," *Proc. Symp. VLSI Tech.*, pp. 15–16, June 1994
- [12] E. Grossar , M. Stucchi , K. Maex and W. Dehaene "Read stability and write-ability analysis of SRAM cells for nanometer technologies", *IEEE J. Solid-State Circuits*, vol. 41, pp.2577, 2006